Master's Thesis of Pharmacy

Regulatory roles of macrophage Cx43 in adipose tissue remodeling and inflammation

February 2023

Graduate School of Pharmacy
Seoul National University
Pharmacology Major

Abhirup Saha

Regulatory roles of macrophage Cx43 in adipose tissue remodeling and inflammation

Advisor Dr. Yun Hee Lee

Submitting a master's thesis of
Pharmacology

December 2022

Graduate School of Pharmacy
Seoul National University
Pharmacology Major

Abhirup Saha

Confirming the master's thesis written by
Abhirup Saha
January 2023

Chair 이 미 옥 (Seal)
Vice Chair 신 영 기 (Seal)
Examiner 이 윤 희 (Seal)

Contents

Abstract

Regulatory roles of macrophage Cx43 in adipose tissue remodeling and inflammation

Abhirup Saha

College of Pharmacy, Pharmacology

The Graduate School

Seoul National University

Adipose tissue macrophages are key contributors in metabolic disorders and inflammation linked to obesity. Macrophages play an important role in adipocyte mitochondrial function, lipid metabolism, and energy production. The processes causing macrophage infiltration and activation in adipose tissue following obesity, however, are largely unresolved. Previous studies have shown that the gap junctional protein connexin 43 (Cx43) is important for macrophage activation and phagocytosis. I explored the macrophage-specific involvement of Cx43 in the pathological remodelling of adipose tissue triggered by a high fat diet (HFD). Cx43 expression was increased in macrophages co-cultured with dying adipocytes in vitro, and also in macrophages affiliated with dying adipocytes in HFD-fed mice adipose tissue. Based

on global gene expression analysis, Cx43−MKO animals were resilient to HFD−induced inflammatory responses in adipose tissue, potentially via P2X7−mediated signalling pathways. HFD−induced macrophage migration in adipose tissue was attenuated in Cx43−MKO mice. Furthermore, Cx43−MKO mice had decreased inflammasome activation in adipose tissues and improved glucose tolerance. These findings show that Cx43 expression in macrophages promotes inflammasome activation, which promotes HFD−induced metabolic dysfunction.

Keywords: adipose tissue remodelling; connexin 43; inflammation; macrophage; obesity

Student Number: 2019−28309

List of Tables:

List of Figures:

Ⅰ. Introduction

1. Obesity and chronic inflammation

Obesity is regarded as a distinguishing trait of the metabolic syndrome [1]. Obesity results from an imbalance between energy intake and expenditure, a positive energy balance [2]. Obesity and its consequences are a growing problem in developed countries. In 2016, Overweight adults aged 18 and up constituted more than 1.9 billion people. Over 650 million of these people were obese as per WHO (https://www.who.int/en/news-room/fact-sheets/detail/obesity-and-overweight) [3].

White adipose tissue undergoes a phenotypic shift as a result of obesity and weight gain, as seen by the emergence of inflammatory, dysfunctional adipocytes and immune cell infiltration in the stromal vascular system [4]. Adipose tissue macrophages (ATMs) are altered by obesity in terms of both quantity and function and tissue distribution. Macrophages can be broadly separated into two subpopulation types based on the expression of various antigens and cytokines: the classically stimulated M1 type and the alternatively activated M2 type [5].

There is significant proof that systemic inflammation and insulin function are strongly impacted by the polarization status of ATMs [6]. Adipocytes release inflammatory mediators and chemoattractant molecules (like MCP-1) in response to metabolic stress that can draw in and activate both resident and non-resident immune cells. These immune cells, specifically macrophages (M)

and T-lymphocytes (i.e., T-cells), are what keep the WAT in an inflammatory state [7].

2. Adipose Tissue Macrophage regulation during obesity

Macrophages are evolutionary conserved phagocytes that were initially identified by Ilya Metchnikoff in the late 19th century [8]. By initiating and then resolving the inflammatory response, they play a crucial part in the immunological response to infections. However, they also play a crucial part in tissue formation as well as in the observation and tracking of tissue changes. They are crucial for preserving tissue homeostasis, removing apoptotic or senescent cells, and restoring the tissue's structural and functional integrity quickly after harm. The metabolic adaptability of macrophages is highlighted by in vitro studies in the context of pro- or anti-inflammatory activation. Depending on the task at hand, macrophages can entirely rewire aspects of their cellular metabolism [9]. In fact, when resident macrophages are lost, the environment's macrophage niches reprogram entering monocytes to take on the transcriptional patterns that characterize the resident population [10, 11]. Tissue macrophage populations' homeostatic metabolic activities seem to be as diversified as their identities, the range of microenvironments they live in, and consequently, the tasks they carry out to preserve homeostasis in order [12]. Using single-cell RNA-seq to examine the stromal-vascular fraction of visceral adipose tissue from an obese human donor, TREM2-expressing human LAM cells made up a distinct cluster that was distinguished by a highly conserved gene signature. Further, TREM2 deletion increased adipose tissue

hypertrophy and induced systemic hypercholesterolemia and glucose intolerance in obese mice. Suggesting that lipid-associated macrophages like TREM2+ macrophages are related in lipid metabolism in adipose tissue and essential for adipose tissue macrophage remodelling [13]. It was shown that ATMs boosted lipid uptake by increasing activation of the lipid transporters CD36 and Msr1 in the perigonadal adipose tissue of obese mice who were on a calorie-restricted diet and losing weight. After a 24-hour acute fast, stromal vascular cells from the perigonadal adipose tissue of HFD obese mice had macrophages that contained genes for lipid synthesis and lipid uptake, storage, and export. Suggestion that fasting or weight loss causes lipolysis in adipose tissue, which is followed by phagocytosis and lipid updating by ATMs [14]. Another study in adipose tissue discovered that a distinct eWAT macrophage acquires mitochondria from adipocytes in vivo via heparan sulfate synthesizing protein Ext1, which is affected under diet-induced obesity [15].

Phagocytosis is regarded as the most important function of macrophages. It allows for the anti-inflammatory expulsion of aged or damaged cells by macrophages and is critical for maintaining homeostasis in tissues where cellular turnover occurs [16]. Adipose tissue macrophages are understood to contribute to adipocyte death by promoting phagocytosis and lysosomal activation of fragmented cellular contents [17]. ATM phagocytosis of adipocyte debris is important in maintaining Adipose tissue homeostasis, adipocyte turnover, and overall tissue health under normal conditions. ATMs CLS formation are thought to clear dead adipocytes generated by chronic tissue expansion in an obese setting, possibly in an attempt to resolve

inflammation [18]. ATMs play a significant role in the clearing of lipid remains from dead fat cells [19, 20]. Thus ATMs impacts adipose tissue function in a wide range of cellular process.

3. ATP Signaling in inflammation

Energy from nourishment is converted into adenosine 5′ −triphosphate (ATP), the body's useable form of chemical energy, through cellular respiration in the mitochondria. Even though the majority of ATP is found inside cells, under some circumstances it is released into the extracellular environment, where it is an important signalling molecule. Numerous studies have demonstrated the significance of ATP in inflammation. Through autocrine/paracrine purinergic signalling, ATP gives qualitative and quantitative information regarding pericellular damage to inflammatory cells [21, 22].

Extracellular ATP and associated purinergic signalling modulate macrophage activation via an autocrine/paracrine mechanism [23]. In rodent models, ATP depletion or purinergic receptor blockade increased survival and improved outcome of sepsis [24]. Active ATP release from inflammatory cells can arise via vesicular exocytosis as well as via connexin or pannexin hemichannels, most notably Connexin−43 (CX43) [25]. It has been proposed that Cx43 co−operates with P2X7R in macrophages, and that together they mediate intercellular communication via gap junction formation influenced by extracellular ATP [26]. Further, CX43 expression in macrophages was found to be critical in controlling ATP release, local and systemic inflammation, and

ultimately survival in a model of abdominal peritonitis via the purinergic receptor [27].

4. Connexin-43 (Cx43) Gap junction

The indispensable components of cell-cell communication include tight junctions, anchoring junctions (adherens, desmosomes, focal adhesions and hemidesmosomes) and communication junctions (gap junctions, pannexins, ion channels, and chemical synapses) [28]. Gap Junctions are clusters of intercellular channels facilitating a direct connection between the cytoplasm of two neighbouring cells to mediate intercellular communication [29]. Multiple isoforms of Gap Junction proteins form channels between the cytoplasm of adjacent cells, allowing the exchange of ions, signalling molecules, and various metabolites between cells of most tissues. Gap junctions channels are formed by paired connexons, each made up of six connexin (Cx) subunits. Cxs play pivotal roles in a wide range of physiological processes, such as differentiation and proliferation, electrical conductivity, neuronal signalling, hormone secretion, and immune functions [30]. Connexin 43 (Cx43), a 43-kDa protein, is the most ubiquitous and critical Gap Junction protein, playing important developmental, regulatory, and pathophysiological roles in many tissues [31]. Connexin-43 expression and TLR activation are linked in monocytes and macrophages. Pam3CSK4, a TLR2 agonist, and LPS from Escherichia coli, a TLR4 agonist, cause connexin-43 expression in a macrophage cell line (RAW 264.7) in ERK/AP-1 dependent way [32] and causes macrophages to release ATP, which then activates purinergic receptor P2X7 [33]. Concurrent to this,

ATP activates P2X7, raising levels of pro-inflammatory cytokines and bacterial burden [33].

5. Purinergic Signaling

Purinergic signalling, a ground-breaking idea first put out by Prof. Geoffrey Burnstock in 1972, refers to the communication between cells via extracellular nucleosides and nucleotides. Plasma membrane P2 purinergic receptors (P2Rs) are ligated and activated by exogenous purine or pyrimidine nucleotides. P2Rs are widely distributed and play a key role in a variety of physiological and pathological reactions, including neurotransmission, hormone release, inflammation, coagulation, and many other processes [34]. There are two sizable families of P2 receptors, purinergic receptors that favour nucleoside di- and triphosphates: P2Y and P2X [35]. P2Y receptors are seven-transmembrane-spanning proteins coupled to G proteins and varyingly linked to an increase in cytoplasmic Ca2+ and a change in intracellular cAMP levels. P2Y1, P2Y2, P2Y4, P2Y6, and P2Y11 are the mammalian receptors, together with newly cloned P2Y12 and P2Y13. P2Y1, P2Y11, P2Y12, and P2Y13 are purinoceptors with purinoceptor selectivity, P2Y6 is a pyrimidinoceptor, while P2Y2 and P2Y4 receptors have mixed selectivity. The ionotropic P2X receptors belong to the second family of purinergic receptors and comprise two transmembrane domains joined by a significant extracellular loop and a variable-length COOH terminal [36].

The sole known physiological ligand for P2XRs is ATP, making them ATP-selective, ligand-gated, cation-selective channels permeable to Na+,

K+, or Ca2+. Several types of mouse and human immune cells express P2XRs. P2XRs can be divided into three categories: fast-desensitizing (P2X1R and P2X3R), slowly desensitizing or non-desensitizing (P2X2R, P2X4R, and P2X7R), and non-functional in native settings (P2X5R and P2X6R)[37]. P2X1R, P2X2R, P2X3R, and P2X4R have low micro-molar ATP affinities, whereas P2X7R has an extraordinarily high activation threshold [38]. P2X7R is distinguished from other P2XRs by the addition of a cation-selective channel as well as the capacity to activate a plasma membrane pathway that permits cellular uptake of external substances [39].

6. Inflammasome Activation by ATP via P2X receptors

Extracellular ATP was first identified as a physiological signal in 1991 that caused macrophages to digest and release IL-1, and it has since become the most frequently utilized and extensively researched signal for inflammasome activation [40].

Numerous studies have been conducted on the activation of NLRP3 by P2X7 in monocytes, macrophages, and dendritic cells. The activation of P2X7 receptors triggers a number of signalling pathways that lead to the activation of the NLRP3 inflammasome. The generation of ROS, the depolarization of mitochondria, the increase in intracellular Ca2+, the reduction of intracellular K+, and the instability of lysosomes are the key P2X7-induced signalling pathways that distinguish out as the most significant events that trigger NLRP3 activation [40-42]. Protein complex called the NLRP3 inflammasome detects the molecular patterns linked to pathogens and danger and processes IL-1 and

IL-18 (PAMPs and DAMPs). According to a number of studies, the development of chronic, metabolic, and degenerative diseases such type 2 diabetes, non-alcoholic steatohepatitis and liver fibrosis, multiple sclerosis, and Alzheimer's disease may all be influenced by NLRP3 [43, 44].

The oligomerization of various NLRP3 subunits, either triggered by various triggers or encouraged by the expression of gain-of-function mutations, initiates the stimulation of the NLRP3 inflammasome. The amino-terminal pyrin domain of the various NLRP3 subunits serves as a seed for attracting and oligomerizing the Apoptosis-Associated Speck-Like Protein (ASC) with Caspase Recruitment and Increased activity Domain (CARD), which forms long oligomeric filaments in a prion-like oligomerization model after NLRP3 oligomerization [45, 46]. Through homotypic CARD-CARD contacts, ASC filaments bring pro-caspase-1 to the inflammasome and encourage caspase-1 activation through close proximity [47]. Interleukin (IL)-1 and IL-18 are two important, powerful pro-inflammatory cytokines that are activated by active caspase-1 [48].

7. Purpose of the current study

Adipose tissue macrophages have crucial role in inducing adipose tissue inflammation. With previous evidences showing connexion-43 mediated ATP leak from macrophages and consequence in activation of inflammasome and inflammatory cytokines. In this current study I investigated the macrophage connexin-43 role in adipose tissue inflammation and metabolic effect. I used a co-culture system of dying adipocytes with adipose tissue macrophages and

a macrophage-specific Cx43 knockout (KO; Cx43-MKO) mouse model to investigate the pathophysiological role of Cx43. Cx43 expression was upregulated in macrophages co-cultured with dying adipocytes, as well as in adipose tissue from mice fed a high-fat diet (HFD). In vitro, Cx43 knockdown decreased extracellular ATP levels as well as inflammatory responses in macrophages. Cx43-MKO mice were resistant to HFD-induced inflammation and glucose intolerance in vivo.

Ⅱ. Materials and Methods

1. Animals

The Institutional Animal Care and Use Committee at Seoul National University examined and approved all animal protocols (SNU-181120-3, SNU-191204-4-1). The Ministry of Food and Drug Safety's standards for the humane treatment and use of laboratory animals were strictly followed in all animal research. The experiments employed male mice. Mice were kept in cages at a constant temperature of 22.1℃ with a 12 hour light/12 hour dark cycle and unrestricted access to food and water. C57BL/6 mice were purchased from Central Lab. Animal Inc. Csf1r-CreER [49] (stock# 019,098, FVB-Tg (Csf1r-cre/Esr1*)1Jwp/J), and Gja1flox/flox (stock #008039, B6.129s7-Gja1tm1Dlg/J) [50] mice were purchased from Jackson Laboratory. Csf1r-CreER mice and Gja1flox/flox mice were crossed to produce inducible macrophage-specific connexion-43 (Cx43) KO mice (Csf1r-CreER/Gja1 flox/flox: Cx43-MKO mice). For wild type (WT) control, Gja1 floxed mice (Gja1flox/flox) without CreER were used. For Cre recombination, Cx43-MKO mice and WT controls were treated with tamoxifen (75 mg/kg/day, Cayman) dissolved in sunflower oil by oral gavage for five consecutive days. Experiments were started 10 days after the last dose of tamoxifen. For HFD experiment, Cx43-MKO and WT mice were fed a 60% fat diet (Research Diet) or normal chow diet (NCD) for 8 weeks (n = 6 per condition: WT-NCD, WT-HFD, Cx43-MKO-NCD, Cx43-MKO-HFD). For intraperitoneal glucose tolerance test and insulin tolerance test, mice were given D-glucose (2 g/kg body weight, 200 mg/ml, Sigma) and insulin (0.75 U/kg body weight, Sigma)

by intraperitoneal injection, respectively, and blood glucose levels were measured at indicated time points (n = 6 per condition).

2. Western Blot Analysis

Cells were lysed in RIPA Lysis and Extraction Buffer (Thermo Fisher Scientific, 89900), which contains PhoSTOP phosphatase inhibitors and SIGMAFAST Protease Inhibitor Cocktail (Sigma, S8820) (Roche, 4906845001). The pro Prep Bead Beater homogenization device was used to homogenize adipose tissues in PRO-PREP Protein Extraction Solution (iNtRON Biotechnology, 17081). Thermo Fisher Scientific's Pierce BCA Protein Assay Kit (23227) and MultiSkan GO (Thermo Fisher Scientific) at 562 nm were used to measure the protein concentration. Protein sample separation on an SDS-PAGE gel was followed by PVDF membrane transfer (Bio-Rad). Membranes were first incubated in a blocking solution (Tris-buffered saline with 0.1% Tween 20 (TBS-T) containing 5% non-fat dry milk or BSA), followed by sequential incubations with primary antibody at 4℃ overnight and horseradish peroxidase-conjugated secondary antibody at room temperature for one hour. The blocking buffer dilutes antibodies. On an SDS-PAGE gel, protein samples were separated, and then they were transferred to a PVDF membrane (Bio-Rad). Membranes were first incubated in blocking buffer (Tris-buffered saline with 0.1% Tween 20 (TBS-T) containing 5% non-fat dry milk or BSA), followed by sequential incubations with primary antibody at 4℃ overnight and horseradish peroxidase-conjugated secondary antibody at room temperature for one hour. A blocking buffer was used to

dilute antibodies [51]. he antibodies used for western blot are listed in Table 1.

3. Quantitative PCR Analysis

For the qPCR analyses, total RNA from each tissue was isolated using TRIzol reagent (Thermo Fisher Scientific) according to the manufacturer' s instructions. High-Capacity cDNA Reverse Transcription kit (Applied Biosystems) was used to synthesize cDNA, and iQ SYBR Green Supermix (Bio-Rad) was used for qPCR reactions. Bio-Rad CFX Connect Real-Time PCR Detection System and Maestro 1.1 software (version 4.1.2433.1219) were applied to acquire qPCR data. Relative expression levels of each gene were calculated using the 2-⊿Ct method. Peptidylprolyl isomerase A was used for normalization [52]. Primers used for qRT-PCR are listed in Table 2.

4. Histology and immunohistochemistry

Adipose tissues were embedded in paraffin after being fixed in 10% formalin (Sigma, H5014) for 24 hours. The tissue blocks with paraffin embedding were sectioned at a thickness of 5 m. Paraffin slices were used for H&E staining and immunostaining. Deparaffinized slices were stained with Clear View H&E Y alcoholic solution for H&E staining (BBC biochemical). Deparaffinized sections were first pre-incubated with the immunohistochemical blocking buffer (PBS containing 3% BSA) for immunostaining. Then, the primary antibody was incubated at 4℃ overnight and the secondary antibody was incubated at room temperature for 1 hour. In the immunohistochemistry blocking buffer, antibodies were diluted. Antibodies

and dilutions used for immunohistochemistry Anti-F4/80 antibody (rat, 1; 100, Serotech) and anti-Cx43 antibody (rabbit, 1:100, Cell Signaling) and goat anti-rabbit Alexa Fluor 488 (Thermo Fisher Scientific; 1:500). DAPI (Sigma, D9542) was used for nuclear counterstaining. Bright-field images were captured using a Nikon Ts2-FL microscope and NIS Elements BR Analysis (version 5.10.00). Immunofluorescence pictures were analyzed using Zeiss LSM800 confocal microscope and Zen software (version 2.0) [51, 53].

5. Stromovascular Cells (SVC) isolation and Flow cytometry

Gonadal Adipose tissues were removed using PBS, minced, and then digested for one hour at 37 degrees Celsius using type II collagenase (2 mg/ml) in KRBB containing 10 mM HEPES (pH 7.4) and 3% BSA. The preparations were centrifuged at 500 g for 5 minutes after being passed through a 300 m mesh. Adipocytes that were floating were aspirated and collected. Red blood cell lysis buffer was treated with pellets containing the stromal vascular (SV) fraction for 5min at room temperature. The pellets were then run through a 40m mesh and recovered by centrifugation at 500g for 5min [20]. Live cells were processed for cell surface marker staining. Antibodies used for flow cytometry analysis were the following: anti-F4/80-APC and CD11c-BV421 (Biolegends). Anti-F4/80-FITC (Biolegends), anti-Cx43 (rabbit, 1:100, Cell Signaling), and goat anti-Rabbit IgG (H+L) secondary antibody Alexa FluorTM 594 (rabbit, 1:100, Invitrogen). Analytic cytometry was performed using BD FACSLyricTM (BD Biosciences) flow cytometers. Raw data were processed using FlowJo software (Tree Star). For the identification of cell types in flow cytometry data, at least 10,000 cells were analyzed per sample.

For macrophage isolation, dissociated adipose tissue was fractionated by magnetic cell sorting (MACS) with anti-F4/80-FITC/anti-FITC-microbeads (Miltenyi Biotech) [54].

6. Cell Culture

C3H10T1/2 mouse embryonic fibroblasts from the American Type Culture Collection (ATCC), Manassas, Virginia, were grown to confluence in growth medium (DMEM supplemented with 10% fetal bovine serum (FBS) and 1% penicillin/streptomycin at 37℃ in a humidified atmosphere with 5% CO2) before being exposed to bone morphogenetic protein 4 (20 ng/ml; R&D Systems, Minneapolis, Minnesota). After that, the cells were exposed to differentiation medium for 3 days (DMEM supplemented with 10% FBS, 1% P/S, 2.5 mM isobutylmethylxanthine, 1 mM dexamethasone, and 1 g/ml insulin), after which they were kept in medium with 1 g/ml insulin for 4 days [53].

Using INTERFERin, Gja1-targeting siRNA (EMU006781, Sigma) was transfected into RAW 264.7 cells for knockdown (Polyplus). Negative controls for siRNA were utilized. Dying adipocytes were produced by keeping C3H10T1/2 adipocytes that had undergone complete differentiation in DMEM with 1 g/ml insulin for 10 days after differentiation. Following, fully differentiated adipocytes obtained from the C3H10T1/2 cells (10 days' post differentiation) were added to each well of 12-well dishes that contained macrophage cultures and incubated 24 hours [55]. ATP levels were measured with an ATP Determination Kit (Invitrogen) after stimulating with lipopolysaccharide (LPS) for 30 min [24], following manufacturer's

instructions. To test the effects of ATP degradation, apyrase (ATP-diphosphohydrolase, 2U/ml, Sigma) [56] was treated before co-culture, and maintained in the media during co-culture with dying adipocytes.

7. Phagocytosis Assay

For long-term imaging, differentiated C3H10T1/2 adipocytes were labeled with 4,4-difluoro-5-(2-thienyl)-4-bora-3a, 4a-diaza-s-indacene3-dodecanoic acid (BODIPY 558/568 C12) (Invitrogen), and macrophages or RAW 264.7 cells were labeled with Vybrant DiO Cell-Labeling Solution (Invitrogen) overnight. BODIPY-labeled C3H10T1/2 cells were detached, added to the DiO-labeled macrophages, and then co-cultured for 12h [20]. To monitor the phagocytosis of the dying adipocytes by the macrophages, live cell imaging was performed every 2 h with Operetta CLS High-Content Analysis System (Perkin Elmer), and the fluorescence intensity of the images was analyzed using Harmony (Perkin Elmer) high-content imaging and analysis software.

8. Immunocytochemistry

For intracellular immunofluorescence staining, cells were fixed in 4% paraformaldehyde (158127, Sigma-Aldrich), permeabilized in 0.1% Triton X-100 (X-100, Sigma-Aldrich), and stained with antibody against Cx43 antibody (rabbit, 1:100, Cell Signaling) DAPI (D9542; Sigma-Aldrich) was used for nucleus counter staining [54]. Immunofluorescence images were captured with a Zeiss LSM800 confocal microscope and analyzed with Zen software (version 2.0).

9. Statistical Analysis

Statistical analyses were performed using GraphPad Prism 7 software (GraphPad Software). Data are presented as mean ± standard errors of the means (SEMs). Statistical significance between two groups was determined by unpaired t-test. Comparisons among multiple groups were performed using a two-way analysis of variance (ANOVA), with Bonferroni post hoc tests to determine p values [51].

Table 1. Antibodies used for Western blot and Immunohistochemistry

Antibody	Host	Company	Catalog #	Dilution
Cx43	Rabbit	Cell Signaling	3512	1:1000(WB) 1:100(IHC)
F4/80	Rabbit	Cell Signaling	30325	1:1000(WB)
	Rat	Serotech	MCA497GA	1:100(IHC)
p-RIP3	Rabbit	Abcam	ab195117	1:1000
RIP3	Mouse	Cell Signaling	15828	1:1000
NLRP3/NLAP3	Mouse	AdipoGen Life Sciences	AG-20B-0014	1:1000
ASC/TMS1/PYCARD	Mouse	Santa Cruz	sc-514414	1:1000
Anti-Caspase1	Mouse	Santa Cruz	sc-56036	1:1000
α/β tubulin	Rabbit	Cell Signaling	2148	1:3000
Goar anti-rabbit IgG, HRP	Goat	Invitrogen	31460	1:3000
Goat anti-mouse IgG,HRP	Goat	Jackson	115-035-174	1:3000
Donkey anti-Rat IgG (H+L) Highly cross-adsorbed Secondary Antibody, Alexa Fluor™ 488	Rat	Invitrogen	A21208	1:100 (IHC)

Table 2. Primers used for qPCR

Reverse primer	Forward primer	Primer
5'-GTT TTC TCC GTG GGA CGT GA-3'	5'-CAG GTC TGA GAG CCC GAA CT-3'	*Gja1*
5'-CCG ACA GCA CGA GGC TTT-3'	5'-CTG GTG TGT GAC GTT CCC ATT A-3'	*Il-1b*
5'-TCT GAC CAC AGT GAG GAA TG-3'	5'-AGT GGC TAA GGA CCA AGA CC-3	*Il-6*
5'-AAG GCA TCA CAG TCC GAG TC-3'	5'-CTG GAT CGG AAC CAA ATG AG-3	*Ccl2*
5'-TCA CCT GCT CCA CTG CCT TGC-3'	5'-GGC AGA GAA GCA TGG CCC AGA A-3	*Il-10*
5'-GTC AAA CTT GCC AGC CTT TCC-3'	5'-ACA ACG TGT CTC CTG GCT ACA AT-3	*P2rx4*
5'-CCC CAC CCT CTG TGA CAT TCT-3'	5'-AGC ACG AAT TAT GGC ACC GT-3	*P2rx7*
5'-TTA CAG GAC ATT GCG AGC AG-3'	5'-GTG GTC TTT GGG AAG GTG AA-3	*Ppia*

Ⅲ. Results

1. Macrophage Expression of Cx43 Was Upregulated in Gonadal White Adipose Tissue of HFD-Fed Mice

Cx43 expression levels were examined in gonadal white adipose tissue (gWAT) of mice fed an HFD for 8 weeks. HFD-induced Cx43 increased level in gWAT was revealed by Western blot analysis **(Figure 1a)**. Furthermore, immunohistochemistry affirmed that macrophages surrounding adipocytes (i.e., crown-like structures) demonstrated significant concentrations of Cx43 expression **(Figure 1b)**. Flow cytometry assessment of gWAT SVCs revealed that HFD feeding stimulated F4/80+ macrophage recruiting process and elevated Cx43 expression in F4/80+ cells **(Figure 1c)**. From this initial observation it can be concluded that with increase in adipose tissue mass due to excess nutrition, macrophage cx43 expression is increased and may play role in regulation of obesity.

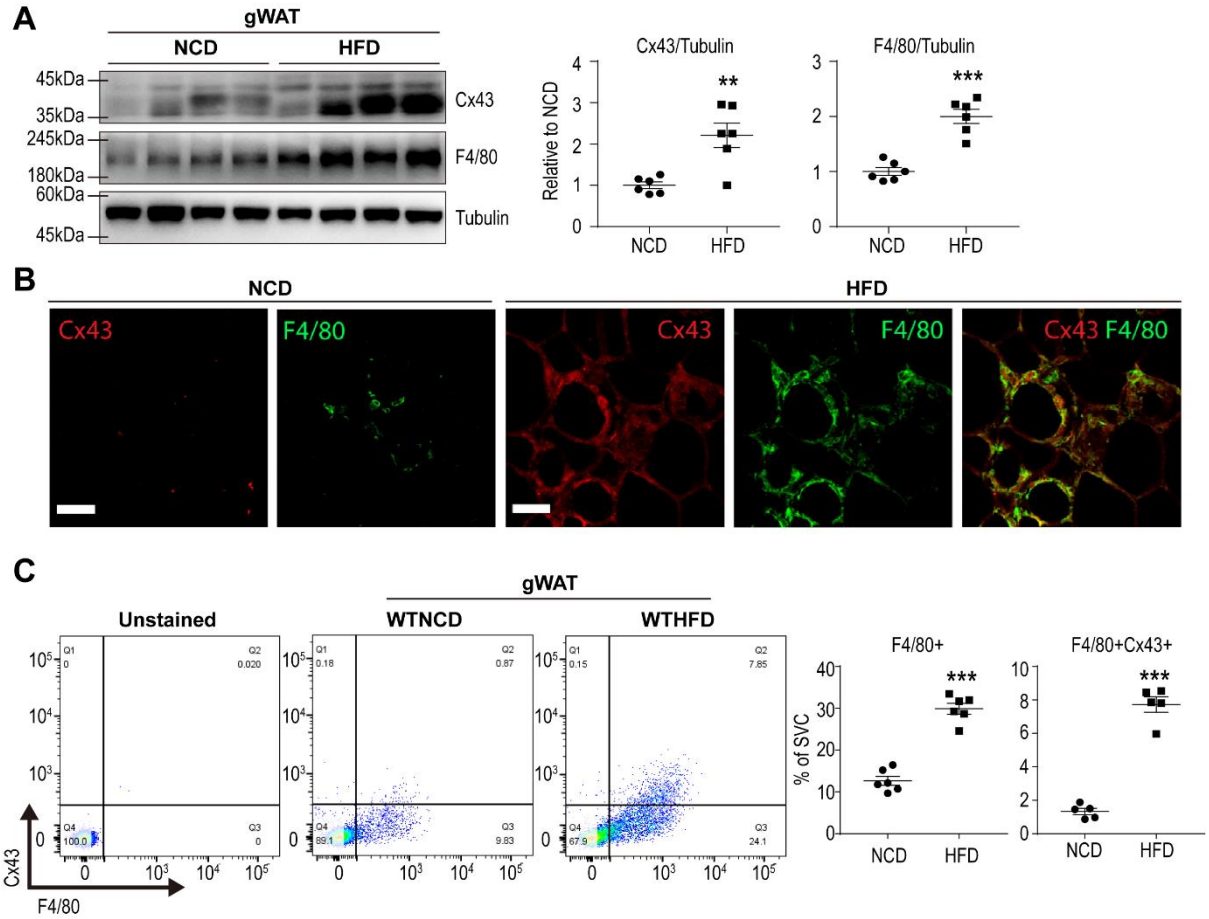

Figure 1. Cx43 is upregulated in gonadal white adipose tissue macrophages of mice by high-fat diet feeding

(a) Immunoblot analysis of Cx43 and F4/80 expression in gonadal white adipose tissue (gWAT) of mice fed normal chow diet (NCD) or high-fat diet (HFD) for 8 weeks (n = 6) (b) Immuno-fluorescence images of paraffin sections of gWAT of mice fed NCD or HFD, stained for Cx43 and F4/80 (c) Flow cytometric analysis of stromovascular cells (SVCs) obtained from gWAT of WT mice fed with NCD or HFD for 8 weeks (n = 6). Unpaired, two-tailed t-tests (**$p < 0.01$, ***$p < 0.001$), each point represents biological replicate. Data are presented as mean ± S.E.M.

2. Macrophages Co-Cultured with Dying Adipocytes Upregulated Cx43 Expression

Adipocyte hypertrophy, adipocyte death, and macrophages surrounding damaged/dying adipocytes characterize HFD-induced adipose tissue remodelling. I established an in vitro system by co-culturing macrophages with dying adipocytes to distinguish the molecular mechanisms of adipose tissue macrophages associated in HFD-induced adipose tissue remodelling (dAC) [54]. Dying adipocytes were procured from continuous cultures of adipocytes differentiated from C3H10T1/2 cells, as previously described. The dying adipocytes were cultured with MACS-isolated adipose tissue macrophages. I used immunoblotting, quantitative PCR, and immunostaining to confirm the upregulation of Cx43 expression in macrophages **(Figure 2a-c)**.

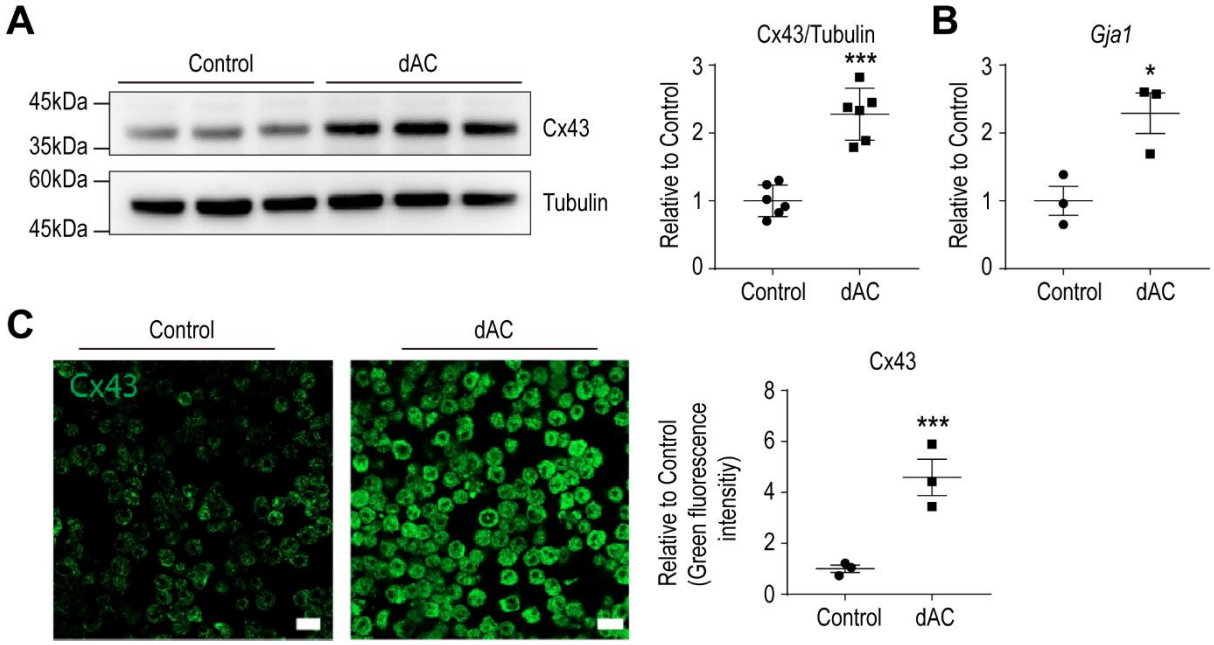

Figure 2. Macrophages co-cultured with dying adipocytes (dAC) upregulate Cx43 expression

(a-b) Immunoblot analysis of Cx43 protein (A) and qPCR analysis of *Gja1* transcript levels (B) in F4/80^{+} macrophages isolated from gWAT co-cultured with dying adipocytes (dAC) for 24 h (A: n = 6, B: n = 3) (c) Immunofluorescence images of Cx43 staining in F4/80^{+} macrophages from gWAT co-cultured with or without dying adipocytes (dAC) for 24 hours (n = 3). Unpaired, two-tailed t-tests (*p < 0.05, ***p < 0.001), each point represents biological replicate. Data are presented as mean ± S.E.M.

3. Cx43 Knockdown Reduced Inflammatory Response of Macrophages Co-cultured With Dying Adipocytes

Cx43 knockdown was analysed in macrophages co-cultured with dying adipocytes. In RAW264.7 cells, I used siRNA to knock down Gja1 (encoding Cx43). I used BODIPY dye to label adipocytes and DIO dye to label macrophages for visualization (Lee 2016). I found that Gja1KD improved the removal of dying adipocytes in macrophages using this co-culture study **(Figure 3a)**. Gja1KD, remarkably, reduced the expression of pro-inflammatory markers while increasing the genes that are involved in anti-inflammatory responses (M2 macrophage markers) **(Figure 3b)**.

Previous research has suggested that Cx43 plays an important role in macrophage pro-inflammatory activation by facilitating ATP release and governing extracellular ATP signalling. As a result, I looked at ATP levels in LPS-treated Gja1KD macrophages and discovered that Gja1KD reduced extracellular ATP levels **(Figure 3c)**. Apyrase treatment reduced the expression of pro-inflammatory cytokines by degrading extracellular ATP (3d). Furthermore, I studied the effect of conditioned media derived from control RAW264.7 cells on dAC **(Figure 3e)**. The conditioned media were found to be sufficient in increasing pro-inflammatory cytokines in Gja1KD RAW264.7 cells **(Figure 3f)**, ATP released through Cx43 hemichannels in the media was found to be a critical signal for inducing inflammatory responses.

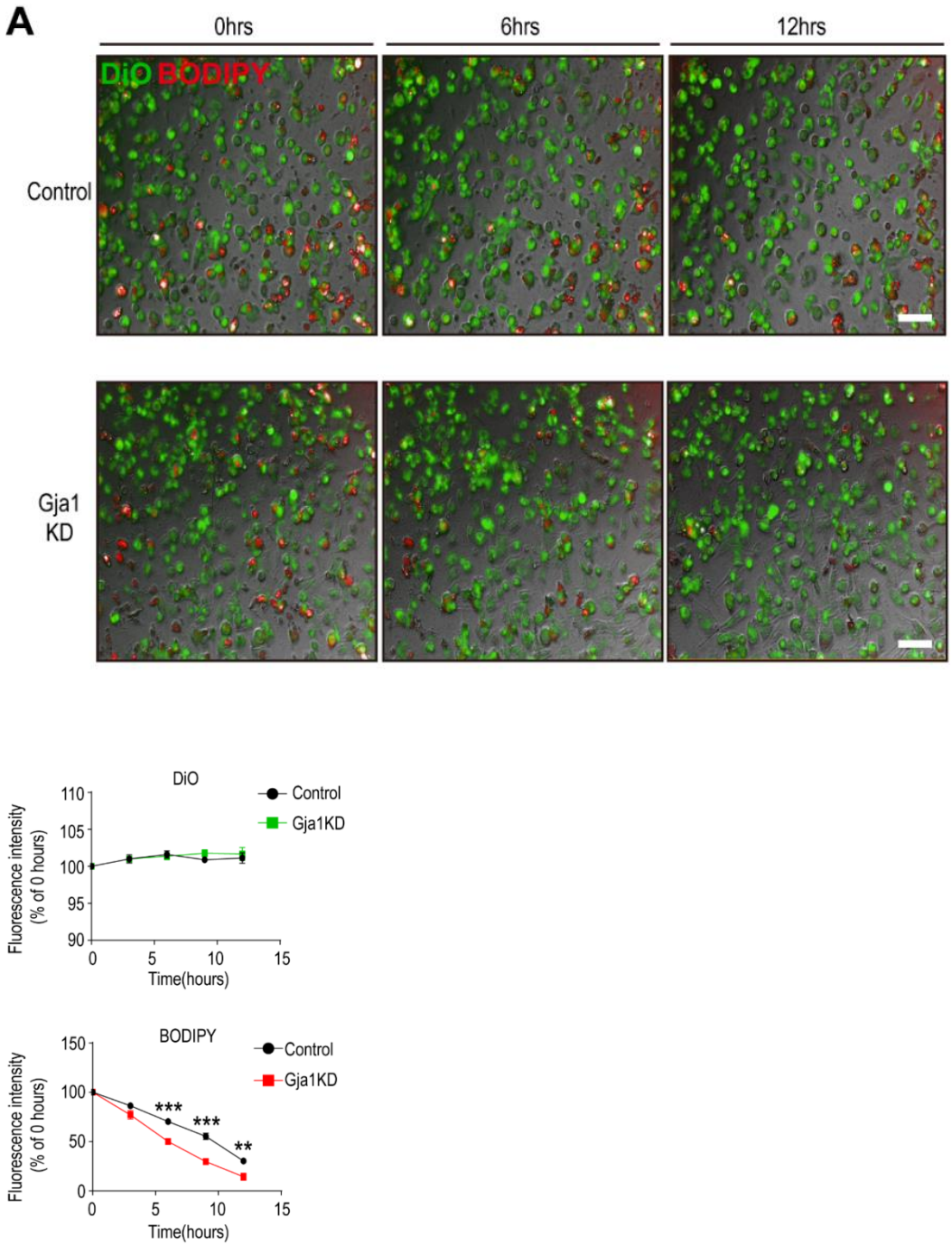
A
0hrs
6hrs
12hrs
DiO BODIPY
Control
Gja1
KD
DiO
Control
Gja1KD
Fluorescence intensity
(% of 0 hours)
110
105
100
95
90
0
5
10
15
Time(hours)
BODIPY
Control
Gja1KD
150
100
50
0
***
***
**

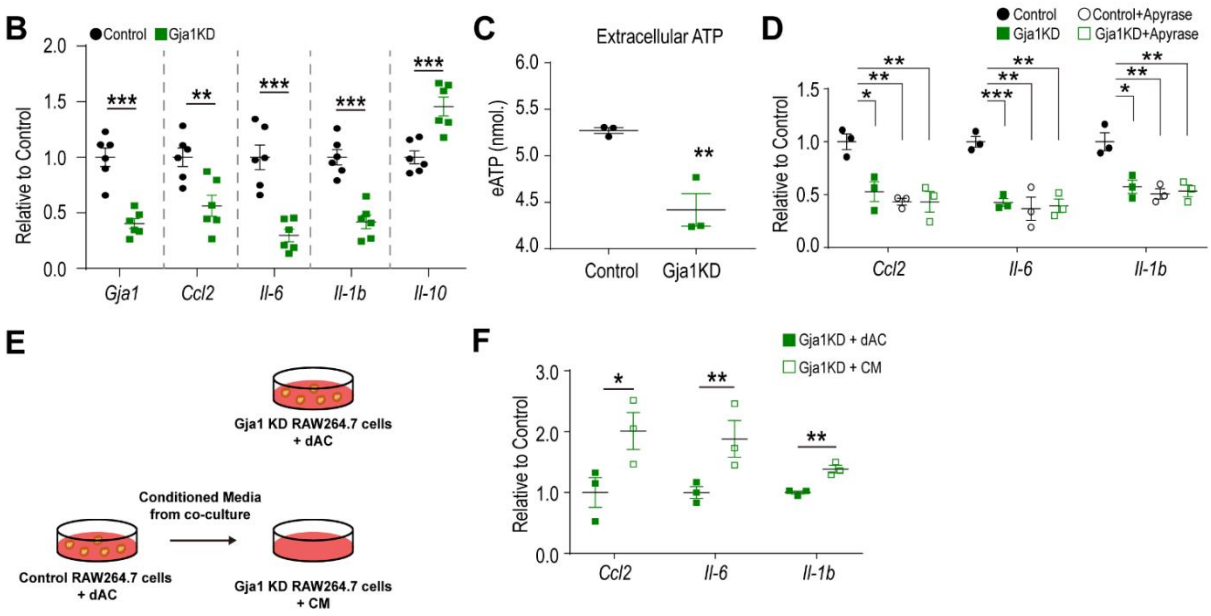

Figure 3. Cx43 knockdown reduces inflammatory responses of macrophages co-cultured with dying adipocytes

(a) Live imaging of RAW264.7 cells transfected with Gja1 siRNA or controls and co-cultured with dying adipocytes (dACs) for 12 h. Adipocytes were tagged with C12-BODIPY (red) and macrophages were stained with DiO (Green) (n = 3) (b) qPCR analysis of Gja1 and inflammatory cytokine markers in RAW264.7 cells transfected with Gja1 siRNA or controls and co-cultured with dACs for 24 h (n = 6) (c) Extracellular ATP level in lipopolysaccharide (LPS)-stimulated RAW 264.7 macrophages treated with Gja1 siRNA or control for 30 min (n = 3) (d) qPCR analysis of inflammatory cytokines in RAW264.7 cells transfected with Gja1 siRNA or controls, and co-cultured with dACs in the presence or absence of apyrase (2U/ml) (n = 3) (e) Schematic diagram illustrating the experimental method used for F. Conditioned media obtained from control RAW264.7 cells co-cultured with dACs were transferred into Gja1KD RAW264.7 cells (f) qPCR analysis of

inflammatory cytokine markers in Gja1 KD RAW264.7 cells co-cultured with dACs (GjaKD + dAC) or exposed to the conditioned media obtained from the control co-cultures (Gja1KD + CM) (n = 3). Unpaired, two-tailed t-tests (*$p < 0.1$, **$p < 0.01$, ***$p < 0.001$). Each point represents biological replicate. Data are presented as mean ± S.E.M.

4. Cx43 KO Protects Mice from HFD-Induced Metabolic Dysfunction, partly by Reducing the Inflammasome Signalling Pathway

I collaborated with Dr Minsoo Noh at College of Pharmacy, Seoul National University for RNA seq Analysis of gWAT from WT and Cx43-MKO mice fed either normal chow or HFD diet. The transcriptomic data indicated purinergic receptors related to inflammasome activation P2rx7, and P2rx4, were elevated in the WT-HFD group (data not shown). Using qPCR, immunoblotting, and immunohistochemical analyses, further confirmed the RNA-seq data at transcript and protein levels. HFD feeding increased P2RX7 and P2RX4 expression levels in the gWAT of WT mice, although not in the gWAT of Cx43-MKO mice, according to qPCR analysis **(Figure 4a)**. Following HFD feeding, Cx43-MKO diminished the accumulation of crown-like structures in gWAT, according to histopathological study of H&E-stained paraffin sections **(Figure 4b)**. Further confirmation that Cx43-MKO reduced HFD-induced recruitment of F4/80+ macrophages came from a Western blot analysis **(Figure 4c)**. When comparing Cx43-MKO mice to WT-HFD-fed mice, qPCR analysis supported the RNA-seq data by showing reduced mRNA expression of pro-inflammatory cytokines in the HFD-fed Cx43-MKO mice **(Figure 4a)**.

P2RX7 signalling in macrophages is known to promote the inflammasome signalling pathway. As a result, after 8 weeks of HFD feeding, MKO mice's gWAT expression of inflammasome markers decreased **(Figure 5a)**. Additionally, FACS analysis revealed that KO mice fed an HFD had fewer pro-inflammatory macrophages (F4/80+CD11c+) **(Figure 5b)**. Cx43-MKO mice

have improved insulin sensitivity and glucose tolerance, according to phenotypic analysis (Figure 5c).

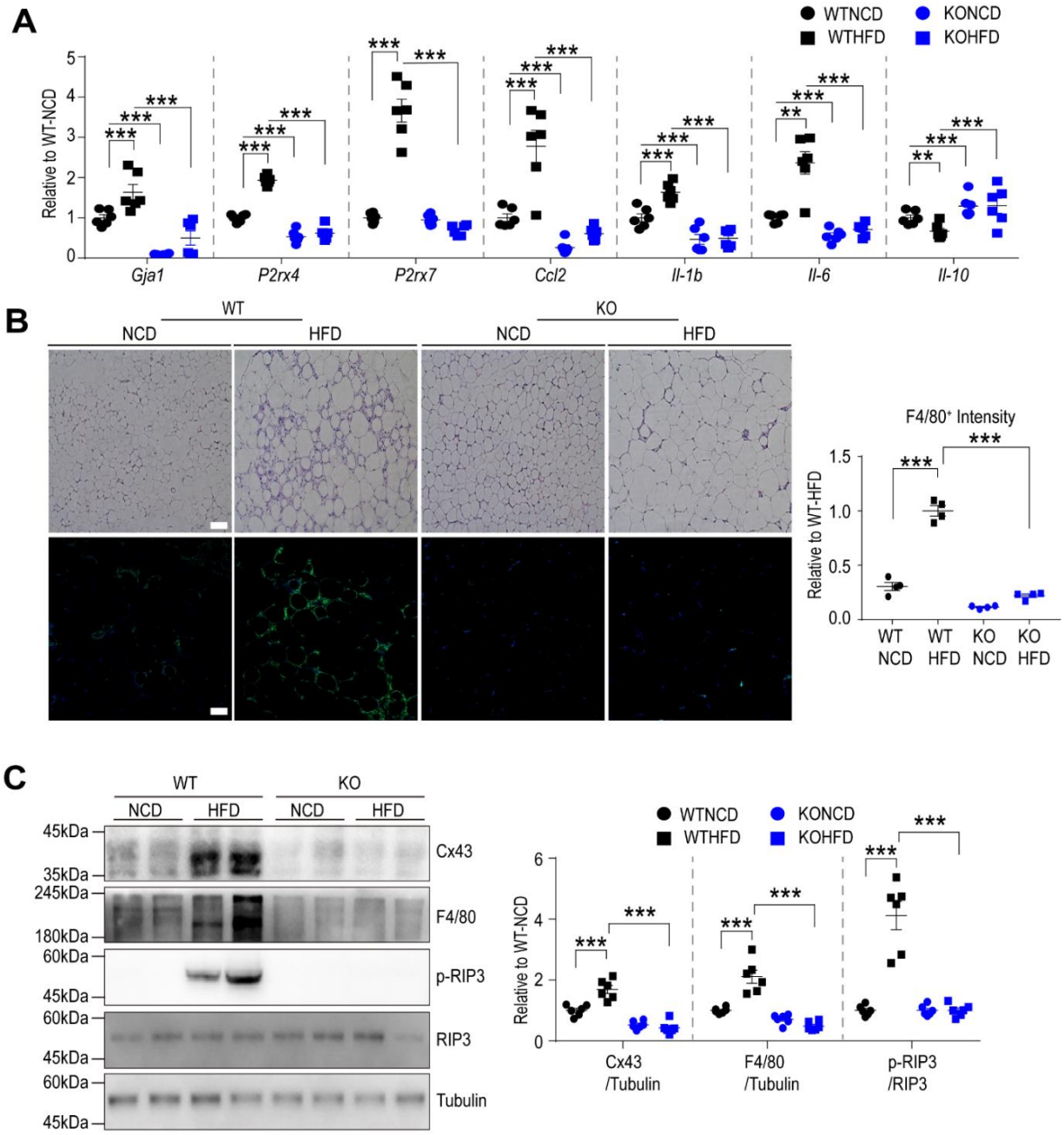

Figure 4. Macrophage-specific Cx43 KO protected mice from HFD-induced inflammation in gonadal white adipose tissue

(a) qPCR analysis of gWAT of WT and Cx43 MKO mice fed with either normal chow diet (NCD) or high-fat diet (HFD) for 8weeks (n = 6). Significant effects of genotype (Gja1: $p = 0.001$, P2rx4: $p < 0.0001$, P2rx7: $p < 0.0001$, Ccl2: $p < 0.0001$, Il-1b: $p < 0.0001$, Il-6: $p < 0.0001$, Il-10: $p < 0.0001$) and

significant effects of diet (Gja1: $p < 0.0001$, P2rx4: $p < 0.0001$, P2rx7: $p < 0.0001$, Ccl2: $p < 0.0001$, Il-1b: $p = 0.0039$, Il-6: $p < 0.0001$, Il-10: $p = 0.0391$) were observed. Significant differences between WT HFD and KO HFD groups were determined by Bonferroni post hoc tests (b) Representative images of H/E and F4/80 stained paraffin sections, and quantification of F4/80 fluorescence intensity in gWAT of WT and Cx43 MKO mice fed NCD or HFD for 8 weeks ($n = 4$). Significant effects of genotype ($p < 0.0001$) and diet ($p < 0.0001$) were observed. Significant differences between WT HFD and KO HFD groups were determined by Bonferroni post hoc tests (c) Immunoblot analysis of gWAT of WT and Cx43 MKO mice fed with either NCD or HFD for 8 weeks ($n = 6$). Significant effects of genotype (Cx43: $p < 0.0001$, F4/80: $p < 0.0001$, p-RIP3: $p < 0.0001$) and significant effects of diet (Cx43: $p < 0.0037$, F4/80: $p = 0.003$, p-RIP3: $p < 0.0001$) were observed. Significant differences between WT HFD and KO HFD groups were determined by Bonferroni post hoc tests. Two-way ANOVA with Bonferroni post hoc tests was used (***$p < 0.001$). Each point represents biological replicate. Data are presented as mean ± S.E.M.

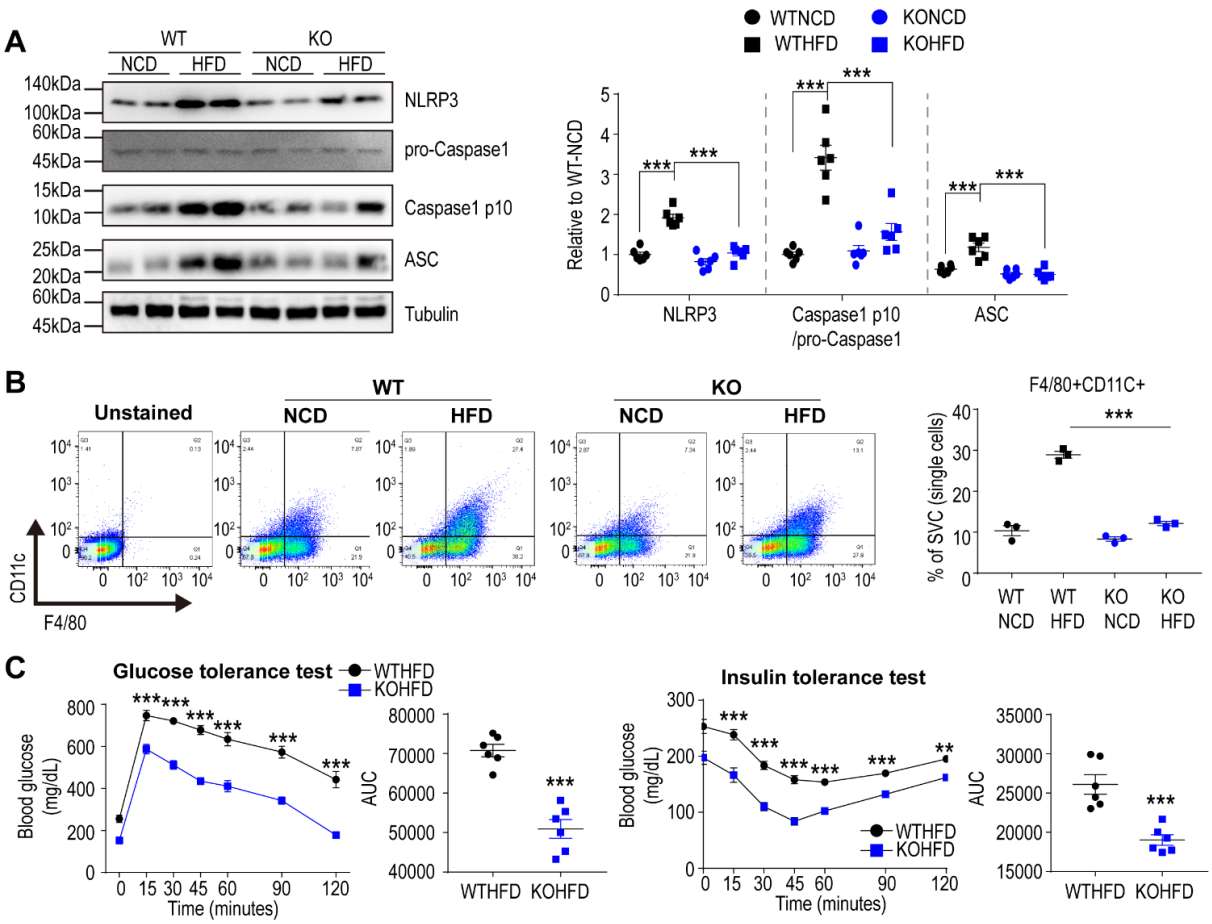

Figure 5. Macrophage-specific Cx43 KO protected mice from HFD induced metabolic dysfunction

(a) Immunoblot analysis of gonadal white adipose tissue (gWAT) of WT and Cx43 MKO mice fed with normal chow diet (NCD) or high-fat diet (HFD) for 8 weeks (n = 6). Significant effects of genotype (NLRP3: $p < 0.0001$, Caspase1 p10: $p < 0.0001$, ASC: $p < 0.0001$) and significant effects of diet (NLRP3: $p < 0.0001$, Caspase1 p10: $p = 0.0001$, ASC: $p = 0.0006$) were observed. Significant differences between WT HFD and KO HFD groups were determined by Bonferroni post hoc tests (b) Flow cytometric analysis of SVCs obtained from gWAT of WT and Cx43 MKO mice fed with NCD or HFD for 8 weeks (n = 3). Significant effects of genotype ($p < 0.0001$) and diet ($p <$

0.0001) were observed. Significant differences between WT HFD and KO HFD groups were determined by Bonferroni post hoc tests (c) Glucose tolerance and insulin tolerance tests of WT and Cx43 MKO mice fed with HFD for 8 weeks (n = 6). Two-way ANOVA with Bonferroni post hoc tests was used in A-B. Unpaired, two-tailed t-tests (**$p < 0.01$, ***$p < 0.001$) were used in C. Each point represents biological replicate. Data are presented as mean ± S.E.M.

Ⅳ. Discussion

Obesity has been associated with a multitude of diseases, including atherosclerosis, cancer, cardiovascular disease, and, most notably, type 2 diabetes [57]. The increase in immune cells in the Adipose tissue of obese people during chronic, low-grade inflammation is primarily attributable to a rise in adipose tissue macrophages (ATMs) [58]. Adipose tissue dysfunction is characterized by adipocyte hypertrophy, immune cell infiltration, and increased expression of pro-inflammatory cytokines [57]. Evidence from recent years has demonstrated that hemichannels do have short-lasting openings that lead in sustained release of cytosolic complexes. Studies have also stated toxins, inflammatory and other pathological changes can spread cytotoxicity to neighbouring cells via this gap junction channels [59]. ATP is an important endogenous metabolite that is prevalent in millimolar concentrations in the cytosol and is minimal enough to permeate at least certain hemichannels. Once ATP is released, it acts as a potent transmitter triggering rises in Ca2+ in neighbouring cells by activation of Purinergic receptors [60] and further NLRP3 inflammasome activation [61].

We discovered that deleting Cx43 from macrophages protected mice from HFD-induced inflammation, improving glucose tolerance and insulin sensitivity. Inflammatory responses in adipose tissue are well-known to be one of primary factors responsible for the onset of over-nutrition-induced metabolic disorders. I hypothesized that in macrophages, Cx43-mediated ATP release and the purinergic receptor P2RX7 signalling pathway are factors that

facilitate over nutrition-induced inflammatory responses. This finding suggests that pharmacologically inhibiting Cx43 could provide a novel therapeutic strategy for obesity-related inflammation and resistance. Adipose tissue macrophages have been identified as the predominant cell types held to account for pro-inflammatory cytokine production and inflammation in this regard. Hypertrophic adipose tissue, for example, is typically associated with pro-inflammatory macrophages and crown-like structures in obese patients. Prior studies employing diet-induced obesity mouse models found that gWAT has greater macrophage infiltration than other depots in distinct anatomical areas, such as subcutaneous and mesenteric WAT [62]. To fully comprehend the impacts of macrophage-specific Cx43 KO on other cell types, including adipocytes, through paracrine processes, more research utilizing single-cell level analyses are required. Further, extracellular ATP signalling, which was not investigated in this study, is also understood to play a role in governing adipocyte function. P2X7 receptor downstream signalling, for example, modulates lipid metabolism and adipogenesis, and P2RX7 knockout affects fat distribution in vivo [63]. I were unable to precisely determine the cell type-specific participation of Cx43/ATP/P2RX7 purinergic signalling in this study. Further research using single-cell level analysis is required to fully understand the consequences of macrophage-specific Cx43 KO on other cell types, including adipocytes, via paracrine mechanisms.

V. Conclusion

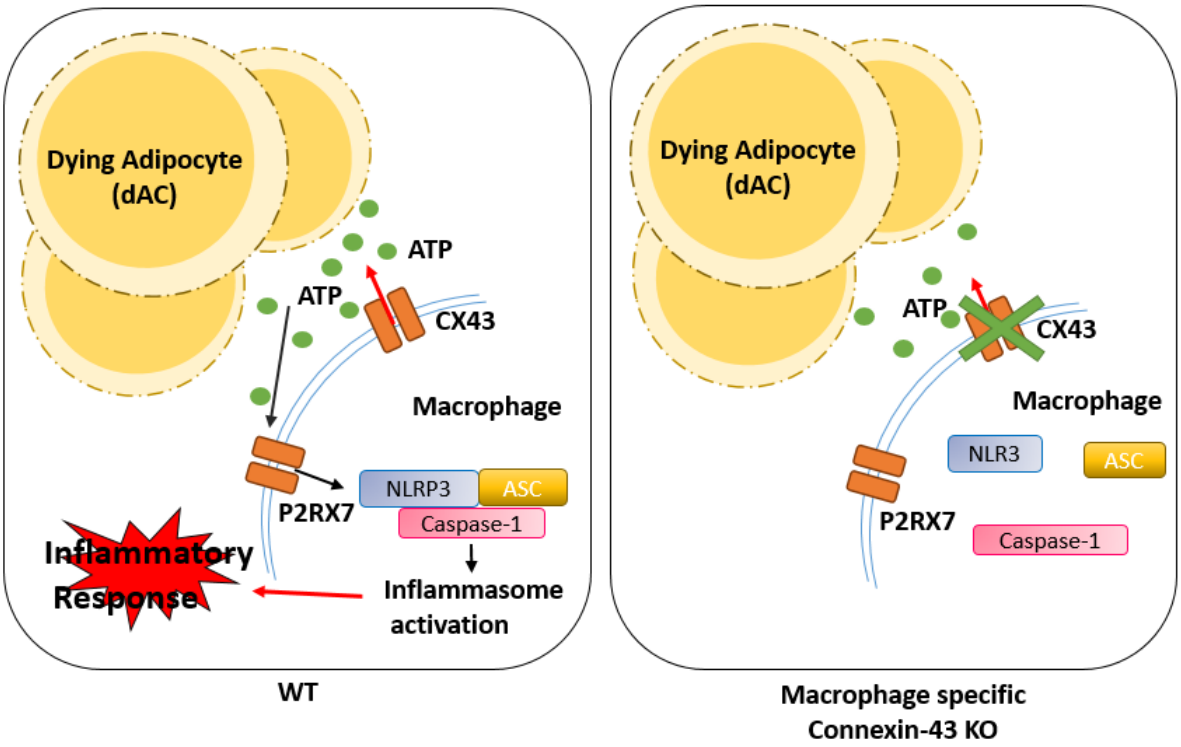

Figure 6. Macrophage-Specific Connexin-43(Cx43) Knockout Protects Mice from Obesity-Induced Adipose Tissue Inflammation.

Current research indicates the crucial part Cx43 plays in macrophage pro-inflammatory activation during HFD-induced mouse adipose tissue remodelling. Mechanistically, P2RX7 may play a role in Cx43-mediated ATP release's ability to trigger autocrine macrophage activation. Understanding the inflammatory processes that occur in adipose tissue and insulin resistance depends on identifying the molecular players that over nutrition causes to activate macrophages.

Ⅵ. References

1. Bassuk, S.S., N. Rifai, and P.M. Ridker, *High-sensitivity C-reactive protein: clinical importance.* Curr Probl Cardiol, 2004. **29**(8): p. 439-93.
2. Krzysztoszek, J., E. Wierzejska, and A. Zielinska, *Obesity. An analysis of epidemiological and prognostic research.* Arch Med Sci, 2015. **11**(1): p. 24-33.
3. Heilbronn, L.K. and L.V. Campbell, *Adipose tissue macrophages, low grade inflammation and insulin resistance in human obesity.* Curr Pharm Des, 2008. **14**(12): p. 1225-30.
4. Hotamisligil, G.S., *Inflammation, metaflammation and immunometabolic disorders.* Nature, 2017. **542**(7640): p. 177-185.
5. Mosser, D.M., *The many faces of macrophage activation.* J Leukoc Biol, 2003. **73**(2): p. 209-12.
6. Patsouris, D., et al., *Ablation of CD11c-positive cells normalizes insulin sensitivity in obese insulin resistant animals.* Cell Metab, 2008. **8**(4): p. 301-9.
7. Olefsky, J.M. and C.K. Glass, *Macrophages, inflammation, and insulin resistance.* Annu Rev Physiol, 2010. **72**: p. 219-46.
8. Kasamatsu, J., *Evolution of innate and adaptive immune systems in jawless vertebrates.* Microbiol Immunol, 2013. **57**(1): p. 1-12.
9. Van den Bossche, J., L.A. O'Neill, and D. Menon, *Macrophage Immunometabolism: Where Are We (Going)?* Trends in Immunology, 2017. **38**(6): p. 395-406.

10. Lavin, Y., et al., *Tissue-resident macrophage enhancer landscapes are shaped by the local microenvironment.* Cell, 2014. **159**(6): p. 1312-26.

11. Mass, E., *Delineating the origins, developmental programs and homeostatic functions of tissue-resident macrophages.* Int Immunol, 2018. **30**(11): p. 493-501.

12. Wculek, S.K., et al., *Metabolism of tissue macrophages in homeostasis and pathology.* Cell Mol Immunol, 2022. **19**(3): p. 384-408.

13. Jaitin, D.A., et al., *Lipid-Associated Macrophages Control Metabolic Homeostasis in a Trem2-Dependent Manner.* Cell, 2019. **178**(3): p. 686-698 e14.

14. Kosteli, A., et al., *Weight loss and lipolysis promote a dynamic immune response in murine adipose tissue.* J Clin Invest, 2010. **120**(10): p. 3466-79.

15. Brestoff, J.R., et al., *Intercellular Mitochondria Transfer to Macrophages Regulates White Adipose Tissue Homeostasis and Is Impaired in Obesity.* Cell Metabolism, 2021. **33**(2): p. 270-+.

16. Poon, I.K., et al., *Apoptotic cell clearance: basic biology and therapeutic potential.* Nat Rev Immunol, 2014. **14**(3): p. 166-80.

17. Cinti, S., et al., *Adipocyte death defines macrophage localization and function in adipose tissue of obese mice and humans.* J Lipid Res, 2005. **46**(11): p. 2347-55.

18. Strissel, K.J., et al., *Adipocyte death, adipose tissue remodeling, and obesity complications.* Diabetes, 2007. **56**(12): p. 2910-8.

19. Lee, Y.H., A.P. Petkova, and J.G. Granneman, *Identification of an adipogenic niche for adipose tissue remodeling and restoration.* Cell Metab, 2013. **18**(3): p. 355-67.

20. Lee, Y.H., et al., *Adipogenic role of alternatively activated macrophages in beta-adrenergic remodeling of white adipose tissue.* Am J Physiol Regul Integr Comp Physiol, 2016. **310**(1): p. R55-65.

21. Cekic, C. and J. Linden, *Purinergic regulation of the immune system.* Nature Reviews Immunology, 2016. **16**(3): p. 177-192.

22. Junger, W.G., *Immune cell regulation by autocrine purinergic signalling.* Nature Reviews Immunology, 2011. **11**(3): p. 201-212.

23. Idzko, M., D. Ferrari, and H.K. Eltzschig, *Nucleotide signalling during inflammation.* Nature, 2014. **509**(7500): p. 310-7.

24. Cauwels, A., et al., *Extracellular ATP drives systemic inflammation, tissue damage and mortality.* Cell Death Dis, 2014. **5**(3): p. e1102.

25. Junger, W.G., *Immune cell regulation by autocrine purinergic signalling.* Nat Rev Immunol, 2011. **11**(3): p. 201-12.

26. Fortes, F.S.A., et al., *Modulation of intercellular communication in macrophages: possible interactions between GAP junctions and P2 receptors.* Journal of Cell Science, 2004. **117**(20): p. 4717-4726.

27. Dosch, M., et al., *Connexin-43-dependent ATP release mediates macrophage activation during sepsis.* Elife, 2019. **8**.

28. Brucher, B.L.D.M. and I.S. Jamall, *Cell-Cell Communication in the Tumor Microenvironment, Carcinogenesis, and Anticancer Treatment.* Cellular Physiology and Biochemistry, 2014. **34**(2): p. 213-243.

29. Wiener, J., D. Spiro, and W.R. Loewenstein, *Studies on an Epithelial (Gland) Cell Junction. Ii. Surface Structure.* J Cell Biol, 1964. **22**(3): p. 587-98.

30. Bosco, D., J.A. Haefliger, and P. Meda, *Connexins: key mediators of endocrine function.* Physiol Rev, 2011. **91**(4): p. 1393-445.

31. Koval, M., S.A. Molina, and J.M. Burt, *Mix and match: investigating heteromeric and heterotypic gap junction channels in model systems and native tissues.* FEBS Lett, 2014. **588**(8): p. 1193-204.

32. Qin, J.L., et al., *TLR-Activated Gap Junction Channels Protect Mice against Bacterial Infection through Extracellular UDP Release.* Journal of Immunology, 2016. **196**(4): p. 1790-1798.

33. Csoka, B., et al., *Extracellular ATP protects against sepsis through macrophage P2X7 purinergic receptors by enhancing intracellular bacterial killing.* Faseb Journal, 2015. **29**(9): p. 3626-3637.

34. Jacobson, K.A. and C.E. Muller, *Medicinal chemistry of adenosine, P2Y and P2X receptors.* Neuropharmacology, 2016. **104**: p. 31-49.

35. Ralevic, V. and G. Burnstock, *Receptors for purines and pyrimidines.* Pharmacological Reviews, 1998. **50**(3): p. 413-492.

36. Khakh, B.S., et al., *International union of pharmacology. XXIV. Current status of the nomenclature and properties of P2X receptors and their subunits.* Pharmacological Reviews, 2001. **53**(1): p. 107-118.

37. Ding, S. and F. Sachs, *Inactivation of P2X2 purinoceptors by divalent cations.* J Physiol, 2000. **522 Pt 2**(Pt 2): p. 199-214.

38. North, R.A., *Molecular physiology of P2X receptors.* Physiol Rev, 2002. **82**(4): p. 1013-67.

39. Di Virgilio, F., et al., *The P2X7 Receptor in Infection and Inflammation.* Immunity, 2017. **47**(1): p. 15-31.

40. Compan, V., et al., *Cell volume regulation modulates NLRP3 inflammasome activation.* Immunity, 2012. **37**(3): p. 487-500.

41. Yaron, J.R., et al., *K(+) regulates Ca(2+) to drive inflammasome signaling: dynamic visualization of ion flux in live cells.* Cell Death Dis, 2015. **6**(10): p. e1954.

42. Lee, G.S., et al., *The calcium-sensing receptor regulates the NLRP3 inflammasome through Ca2+ and cAMP.* Nature, 2012. **492**(7427): p. 123-+.

43. Heneka, M.T., M.P. Kummer, and E. Latz, *Innate immune activation in neurodegenerative disease.* Nat Rev Immunol, 2014. **14**(7): p. 463-77.

44. Swanson, K.V., M. Deng, and J.P. Ting, *The NLRP3 inflammasome: molecular activation and regulation to therapeutics.* Nat Rev Immunol, 2019. **19**(8): p. 477-489.

45. Schmidt, F.I., et al., *A single domain antibody fragment that recognizes the adaptor ASC defines the role of ASC domains in inflammasome assembly.* Journal of Experimental Medicine, 2016. **213**(5): p. 771-790.

46. Lu, A., et al., *Unified polymerization mechanism for the assembly of ASC-dependent inflammasomes.* Cell, 2014. **156**(6): p. 1193-1206.

47. Boucher, D., et al., *Caspase-1 self-cleavage is an intrinsic mechanism to terminate inflammasome activity.* Journal of Experimental Medicine, 2018. **215**(3): p. 827-840.

48. Broz, P. and V.M. Dixit, *Inflammasomes: mechanism of assembly, regulation and signalling.* Nat Rev Immunol, 2016. **16**(7): p. 407-20.

49. Qian, B.Z., et al., *CCL2 recruits inflammatory monocytes to facilitate breast-tumour metastasis.* Nature, 2011. **475**(7355): p. 222-5.

50. Rios, M., et al., *Conditional deletion of brain-derived neurotrophic factor in the postnatal brain leads to obesity and hyperactivity.* Mol Endocrinol, 2001. **15**(10): p. 1748-57.

51. Cho, Y.K., et al., *STK3/STK4 signalling in adipocytes regulates mitophagy and energy expenditure.* Nat Metab, 2021. **3**(3): p. 428-441.

52. Choi, Y.S., et al., *Synthesis and Evaluation of Neuroprotective Selenoflavanones.* Int J Mol Sci, 2015. **16**(12): p. 29574-82.

53. Kim, S.N., et al., *Connexin 43 is required for the maintenance of mitochondrial integrity in brown adipose tissue.* Scientific Reports, 2017. **7**.

54. Cho, Y.K., et al., *MicroRNA-10a-5p regulates macrophage polarization and promotes therapeutic adipose tissue remodeling.* Mol Metab, 2019. **29**: p. 86-98.

55. Kwon, H.J., et al., *The contribution of arachidonate 15-lipoxygenase in tissue macrophages to adipose tissue remodeling.* Cell Death Dis, 2016. **7**(6): p. e2285.

56. Kruse, R., et al., *IL-8 and global gene expression analysis define a key role of ATP in renal epithelial cell responses induced by uropathogenic bacteria.* Purinergic Signal, 2014. **10**(3): p. 499-508.

57. Palma, G., et al., *Adipose Tissue Inflammation and Pulmonary Dysfunction in Obesity.* Int J Mol Sci, 2022. **23**(13).

58. Weisberg, S.P., et al., *Obesity is associated with macrophage accumulation in adipose tissue.* Journal of Clinical Investigation, 2003. **112**(12): p. 1796-1808.

59. Spray, D.C., et al., *Gap junctions and Bystander Effects: Good Samaritans and executioners.* Wiley Interdiscip Rev Membr Transp Signal, 2013. **2**(1): p. 1–15.

60. Pubill, D., et al., *ATP induces intracellular calcium increases and actin cytoskeleton disaggregation via P2x receptors.* Cell Calcium, 2001. **29**(5): p. 299–309.

61. Zheng, D., T. Liwinski, and E. Elinav, *Inflammasome activation and regulation: toward a better understanding of complex mechanisms.* Cell Discov, 2020. **6**: p. 36.

62. van Beek, L., et al., *The limited storage capacity of gonadal adipose tissue directs the development of metabolic disorders in male C57Bl/6J mice.* Diabetologia, 2015. **58**(7): p. 1601–9.

63. Beaucage, K.L., et al., *Loss of P2X7 nucleotide receptor function leads to abnormal fat distribution in mice.* Purinergic Signal, 2014. **10**(2): p. 291–304.